

# Heat Capacity Setup for Superconducting Bolometer Absorbers below 400 mK

V. Singh · S. Mathimalar · N. Dokania ·  
V. Nanal · R. G. Pillay · S. Ramakrishnan

Received: 14 November 2013 / Accepted: 29 December 2013 / Published online: 11 January 2014  
© Springer Science+Business Media New York 2014

**Abstract** A calorimeter set up with very low heat capacity ( $\sim 20$  nJ/K at 100 mK) has been designed using commercial Carbon based resistors. This calorimeter is used to determine the heat capacity of small samples of superconducting bolometer absorbers. In particular, we present heat capacity studies of Tin, a bolometer candidate for Neutrinoless Double Beta Decay in  $^{124}\text{Sn}$ , in the temperature range of 60–400 mK.

**Keywords** Calorimeter · Specific heat · Tin Debye temperature

## 1 Introduction

The performance of bolometers as thermal radiation detectors is determined by its efficiency to measure the change in temperature against the thermodynamic energy fluctuation present in the system. The heat capacity of the absorbing material is the most crucial aspect in a calorimetric particle detector construction as the intrinsic

---

V. Singh · S. Mathimalar · N. Dokania  
Homi Bhabha National Institute, Anushaktinagar, Mumbai 400094, India

V. Singh · S. Mathimalar · N. Dokania  
India based Neutrino Observatory, Tata Institute of Fundamental Research,  
Mumbai 400005, India

V. Nanal (✉) · R. G. Pillay  
Department of Nuclear and Atomic Physics, Tata Institute of Fundamental Research,  
Mumbai 400005, India  
e-mail: nanal@tifr.res.in

S. Ramakrishnan  
Department of Condensed Matter Physics and Material Sciences,  
Tata Institute of Fundamental Research, Mumbai 400005, India

resolution of a calorimeter is strongly dependent on its heat capacity [1]. Bolometer absorbers when operated at temperature close to absolute zero have extremely small heat capacity and are sensitive to even small amounts of energy deposited in a large absorber. In addition, bolometers provide a wide range of energy threshold, sensitivity to even non-ionizing particle events and have found attractive applications in rare event studies like Neutrinoless Double Beta Decay (NDBD) study [2,3] or Dark Matter search [4,5].

Superconductors with high Debye temperatures are ideal candidates for calorimetric particle detectors as the electronic heat capacity falls off exponentially below their transition temperature  $T_c$  and only the lattice contribution to heat capacity remains. At low temperature detectors constructed using superconductors are expected to offer energy resolution comparable to that of diamagnetic insulating absorbers. Although large size calorimetric detectors constructed from diamagnetic insulators have found attractive applications [3–7], the use of superconducting absorbers has been limited only to micro-calorimeters. It is reported that the spectral resolution of superconducting bolometers is limited by the incomplete thermalization of energy in the absorber materials. This has been attributed to energy trapping by quasiparticles with long lifetime in superconductors [8,9]. In the low temperature limit the average recombination lifetime of the quasiparticle is given by [10]

$$\tau_r = \frac{\tau_0}{\sqrt{\pi}} \left( \frac{k_B \cdot T_c}{2\Delta} \right)^{5/2} \sqrt{\frac{T_c}{T}} \exp\left(\frac{\Delta}{k_B T}\right) \quad (1)$$

where  $T_c$  and  $\Delta$  are the critical temperature and the energy gap of the superconductor, respectively. The  $\tau_0$  is the characteristic electron–phonon interaction time and is material dependent. Contrary to the prediction of Eq. (1), recent measurements by Visser et al. [11] in Aluminum show that the  $\tau_r$  saturates to about 2.2 ms below 160 mK. Other superconductors such as Pb, Ta and Sn have a much lower value of  $\tau_0$  (<2.5 ns [10]) compared to Al ( $\tau_0 = 438$  ns). Here, because of the smaller  $\tau_0$  a lower saturation value of quasiparticle lifetime  $\tau_r$  is expected and complete thermalization may be possible, which should lead to improved energy resolution in these bolometers. The long lifetimes of quasiparticles may arise due to the internal trapping process resulting from internal defects or magnetic impurities which should also reflect in anomalous heat capacity at low temperature. An extensive review by Phillips [12] gives a compilation of low temperature heat capacity data for metals but the calorimetric data for most of the superconductors exist only above 300 mK, except in few cases like Sn, Al, Re where the heat capacity in the superconducting phase has been measured down to  $\sim 150$  mK.

Though superconductors like Re, Mo, Zr, Zn, Va, Sn offer similar low heat capacity, only Sn microcalorimeter has been shown to give an excellent resolution till date [13, 14]. An effort has been initiated to make a large size Tin bolometer ( $3 \times 3 \times 3$  cm<sup>3</sup>) which will be used to study NDBD in <sup>124</sup>Sn [15]. It is important to measure and quantify the heat capacity of Tin absorbers and all other materials used in construction of bolometers (sensor, heater, epoxy) to eliminate the possibility of anomalous heat capacity degrading the resolution of a bolometer. With this motivation the heat capacity of high purity Tin samples has been investigated in the range of 60–400 mK.

## 2 Relaxation Calorimetry Setup

Thermal relaxation calorimetric technique [16–19] was used to measure the heat capacity. In this method the specimen is disturbed from its equilibrium temperature ( $T_0$ ) by supplying a known time-dependent input power ( $P(t)$ ) and measuring the temperature response, which is governed by the following relation

$$\frac{d}{dt} \left( \int_{T_0}^{T_0+\Delta T} C(T) dT \right) + \int_{T_0}^{T_0+\Delta T} k(T) dT = P(t) \quad (2)$$

where  $C(T)$  is the heat capacity of specimen and  $k(T)$  is the thermal conductance of the link between the specimen and temperature bath. For small  $\Delta T$ , the quantities  $C(\bar{T})$  and  $k(\bar{T})$  can be assumed to be constant, and the temperature response after turning off the heating power can be approximated as

$$T(t) = T_0 + \Delta T_{max} \cdot \exp(-t/\tau) \quad (3)$$

where  $\Delta T_{max}$  is the maximum temperature change due to input power and  $\tau$  is the relaxation time of the system. It can be easily shown that the relaxation time is dependent on the heat capacity of the system and the thermal conductance ( $k_w$ ) of weak heat link.

$$\tau = C/k_w. \quad (4)$$

倾向单tau?

If the thermal contact between the sample and platform is poor the temperature relaxation curve is characterized by a second exponential and is called the ‘lumped  $\tau_2$  effect’ [20,21]. However, if the thermal conductivity of the sample ( $k_s$ ) is poor compared to the thermal conductance ( $k_w$ ) of the weak heat link the temperature relaxation can be represented by a sum of an infinite series of exponentials. This has been discussed in Refs. [17,22]. In both these cases the data analysis is complicated as the temperature relaxation deviates from a single exponential.

To measure the heat capacity of small sample superconductors it is necessary to realize an addendum which is as small as possible compared to the heat capacity of the specimen. The setup for measuring heat capacity comprises a sapphire platform (15 mm  $\times$  12 mm  $\times$  0.4 mm) on which the Tin samples were mounted. The platform is suspended by insulated NbTi wires ( $\phi = 125 \mu\text{m}$ ) inside a Copper box which acts as thermal bath (Fig. 1).

The weight of the sapphire platform is  $\sim 300$  mg and owing to its very high Debye temperature (1,024 K) has negligible contribution to the measured heat capacity at low temperatures. Employing a one-dimensional model for heat flow and assuming that the sample has infinite thermal conductivity when compared to the conductivity of weak thermal links, Bachmann et al. [17] have shown that about one third of the wire heat capacity should be included as an addendum. Hence, superconducting NbTi wires were used as weak thermal links for minimizing the electronic heat capacity.

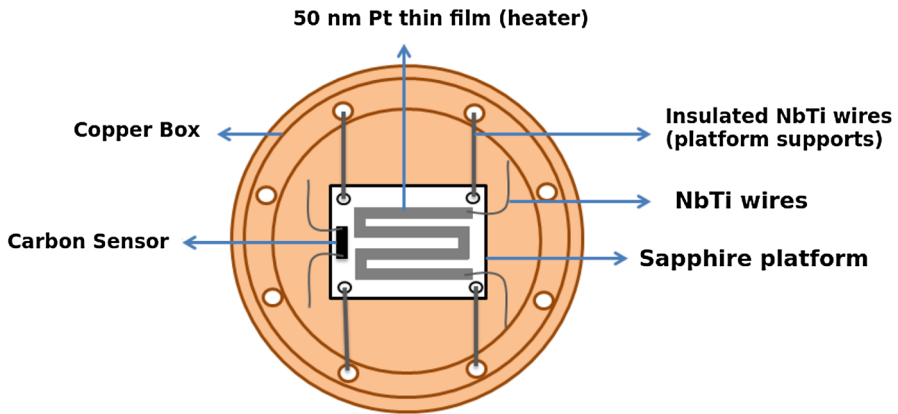


**Fig. 1** Schematic of heat capacity setup. The NbTi wires along with the platform support wires constitutes weak thermal link to the temperature bath. Superconducting wires are chosen to reduce the contribution of addenda. The sample is mounted on top of the platform sapphire. The Pt heater is on the opposite side (Color figure online)

The use of other weak thermal links like Constantan, Manganin and Pt–W wires which have anomalous high heat capacity at low temperatures due to presence of magnetic elements in it, was ruled out for these measurements.

A platinum thin film ( $t \sim 50$  nm;  $wt \sim 48$   $\mu$ g) was deposited on the sapphire platform to obtain a heater with negligible heat capacity (estimated to be  $\sim 0.16$  nJ/K at 100 mK). Platinum was chosen because of its resistance to oxidation and good adhesion to sapphire when compared to Gold. It was verified that the heater resistance ( $\sim 550$   $\Omega$ ) was constant in the temperature range of measurements. Thin NbTi ( $\sim 80$   $\mu$ m) wires were bump bonded to the Pt heater using Indium dots. The NbTi wires were prepared by etching 125  $\mu$ m Copper clad NbTi wire in nitric acid. The ends of the wires were waxed before it was dipped in nitric acid to preserve an extremely small amount of Copper on the ends. This was done as NbTi by itself is not wetted by Indium and the Copper ends facilitate better electrical contact when bump bonded. Also the use of superconducting wires ensured that there is no heat dissipation on the lead wires when the excitation current flows through it.

A Carbon based thermometer has been used as the sensor. The use of Carbon composition resistor from Ohmite Manufacturing Co. for milli-Kelvin thermometry was suggested by Samkharadze et al. [23]. They have shown that this resistor has good thermal contact to its surrounding and can be used down to 5 mK. Following Samkharadze et al. the phenolic package was removed from a 10  $\Omega$  resistor and the resistor was thinned down to 0.4 mm. The sensor was stuck to the sapphire platform using a thin layer of fast setting Araldite. Copper ended NbTi wires were attached to the two ends of thinned Carbon resistor using a small amount of Silver paste. One of the popular alternatives for low temperature sensor is a Ruthenium Oxide ( $\text{RuO}_2$ ) based chip resistor. We tried using a commercial Dale  $\text{RuO}_2$  chip resistor (1 k $\Omega$  at room temperature; mass  $\sim 1.5$  mg) as a sensor. However, it was found out that the heat capacity measured with  $\text{RuO}_2$  sensor had a Schottky ( $\sim 1/T^2$ ) contribution at milli-Kelvin temperatures and this significantly overwhelmed the heat capacity of

gram sized Tin samples below 150 mK. Similar observations have been reported in the literature [19] and the contribution has been attributed to the magnetic impurities present in the alumina substrate of RuO<sub>2</sub>. This limits the use of RuO<sub>2</sub> chip resistor for heat capacity measurement for small samples of superconductors below 150 mK. As we shall show, no such Schottky contribution is observed for the Carbon sensor used in our setup.

The measurements were carried out in a high cooling power (1.4 mW at 120 mK) cryogen-free dilution refrigerator setup at TIFR, Mumbai [24]. The whole setup is enclosed within a Faraday cage for EMI shielding. The dilution unit has an additional option of top loading probe insert which gets connected to the mixing chamber and facilitates easy sample changes in cold condition. The heat capacity setup was attached to the probe insert. The Carbon sensor was calibrated against a secondary resistance thermometer attached to the mixing chamber of the dilution refrigerator.

The heater current was supplied by a Keithley 220 programmable current source. The d.c. lines were filtered using a 3-stage RC filter (located at room temperature) with 30 ms time constant to suppress the high frequency noise emanating from the current source unit that could heat up the platform. This filter time constant ( $\sim$ ms) is much smaller than the measured time constant ( $\sim$ few secs) and hence did not affect the heat capacity measurement. An AVS 47B a.c resistance bridge was used to measure the change in the resistance with a sampling rate of 1.5 samples/s. To prevent self heating of the sensor a low excitation voltage was used such that the power dissipated in the sensor was less than 1 pW. The heater power was chosen such that the  $\Delta T$  was within 5% of the base temperature  $T_0$ . The base temperature  $T_0$  was independently controlled and multiple measurements of temperature decay curve were made at each base temperature (Fig. 2). The decays were single exponential and we did not observe any ‘lumped  $\tau_2$  effect’ for our samples. We have also analyzed the data using dual slope method [25] and found no difference as compared to the method of exponentially fitting the temperature decay. The sensor saturated below 60 mK indicating that the thermal contact of the platform to the cold bath is extremely weak and platform is unable to cool down in presence of background heating. The background heating could be due to the hanging arrangement of the platform which can capture the vibrations of the probe insert of the dilution refrigerator on which it is mounted. Johnson noise from higher

单tau  
two tau?

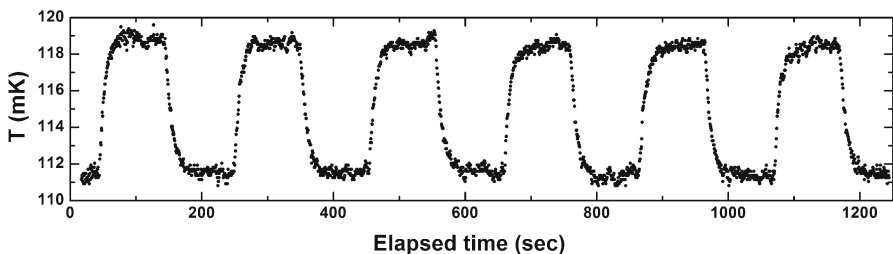


**Fig. 2** A typical picture of the measured temperature variation of the Carbon sensor in response to a square-wave current supplied to the heater on the sapphire platform (see text for details). Each of the thermal relaxation curve is fitted to a single exponential to obtain a time constant. The relaxation time constant  $\tau$  is obtained by doing a weighted average of time constants of all curves

stages of the dilution refrigerator radiated down the electrical lines of the thermometer and heater can be another reason for overheating. The heat capacity setup is mounted inside a copper box which is closed from all sides except for few holes for electrical connection and evacuation. The copper box and a thermal shield at 50 mK stage of the dilution refrigerator ensure that the radiation heat load from higher stages of dilution refrigerator is minimized.

To get the specific heat of Tin, heat capacity of two different masses ( $M_1 = 3.0826$  and  $M_2 = 2.5819$  g) of high purity (99.999 %) Tin were measured. The samples were stuck on the sapphire platform using a thin layer of Apiezon N-grease. The difference between the two measured heat capacities, normalized by the mass difference, eliminates all systematic errors and contribution from the addenda. The subtraction method does not completely eliminate the heat capacity contribution from the N-grease which was used to stick the sample on the platform. Since only a thin layer of N-grease was applied it is difficult to exactly quantify its amount. However, since both the samples have similar surface area, it was assumed that the amount of N-grease used in both the cases would be nearly equal.

### 3 Thermal Conductance ( $k_w$ )

It is important to accurately measure the thermal conductance of the weak heat link to the cold bath as it changes appreciably with temperature. It is calculated from the applied power  $P$  and measured  $\Delta T$  according to the relation

$$k_w = \frac{P}{\Delta T} \quad (5)$$

It can easily be shown that for small  $\Delta T$  the criteria,  $k_w(T) = k_w(\bar{T})$  and  $C(T + \Delta T) = C(\bar{T})$ , are satisfied for the above relation to hold good. Figure 3 shows the measured conductance of the weak heat link for both the Tin samples. The measured conductance can be approximated to the power law  $k = a T^b$  and the fit values obtained are

$$k_w(T) = 0.32 T^{2.06} \mu\text{W/K} \quad (6)$$

From this fit, the absolute thermal conductivity of NbTi wire is estimated and is shown in the inset of Fig. 3. Here it is assumed that the NbTi wires provide parallel paths for heat leak to the thermal bath for the arrangement given in Fig. 1. The systematic error in thermal conductivity due to uncertainties in length estimation of NbTi wirings for sensor and heater is less than 10%. The lattice conductivity of polycrystalline NbTi deviates from the Debye model at low temperatures where  $k \propto T^3$  dependence is expected. The measured  $T^2$  dependence can be better understood in the framework of ‘glass-like’ lattice vibrations in NbTi at low temperatures [26] and is consistent with the thermal conductivity of NbTi wires as measured by Olson [27]. Therefore, in the present case the main contribution to the thermal conductance is only due to the NbTi wires. The measured thermal conductance to the bath and the fact that only a single

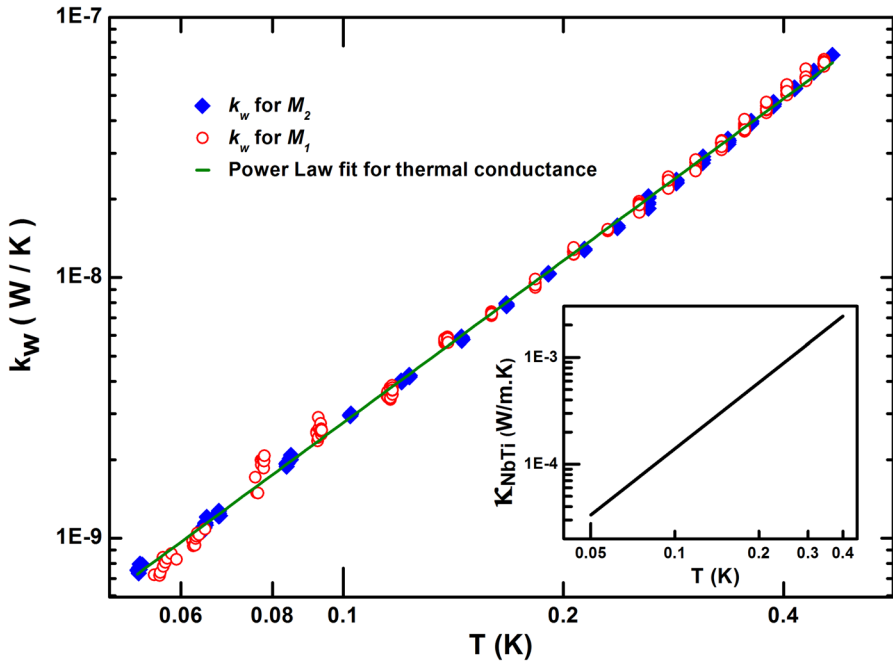


**Fig. 3** The measured thermal conductance of the weak heat link for different measurement runs and its power law ( $k = a T^b$ ) fit. Estimated thermal conductivity of NbTi wire is also shown in the *inset* (see text for details) (Color figure online)

exponential decay time constant was observed implies that the thermal conductance between sample and the platform is much larger than the  $k_w$ . The thermal conductance also serves as a diagnostic measure to ensure that the mounting arrangement is identical between runs.

#### 4 Specific Heat of Tin

The Tin sample plus platform was heated to an equilibration temperature  $\Delta T$  above a constant reference temperature  $T_0$  and then the heater was turned off. The temperature decay was fitted to a single exponential to obtain the time constant. The masses have been chosen to ensure that the  $\tau$  is of the order of 5–15 s in the temperature range of measurement. The heat capacity of the sample was extracted using Eqs. (3) and (4). Heat capacity data for both the samples are shown in Figs. 4 and 5, where the ratio of  $C/T$  is plotted against  $T^2$ .

The straight line fit to the data shows that the measured heat capacity has only linear and cubic dependence on absolute temperature. There is no Schottky like term ( $\sim T^{-2}$ ) which suggests the absence of any magnetic impurity in the sample and the constituents of the platform. The heat capacity values obtained from the fit are

$$C_{M_1} + C_{addenda} = (210 \pm 5)T + (9502 \pm 128)T^3 \text{ nJ/K} \quad (7)$$

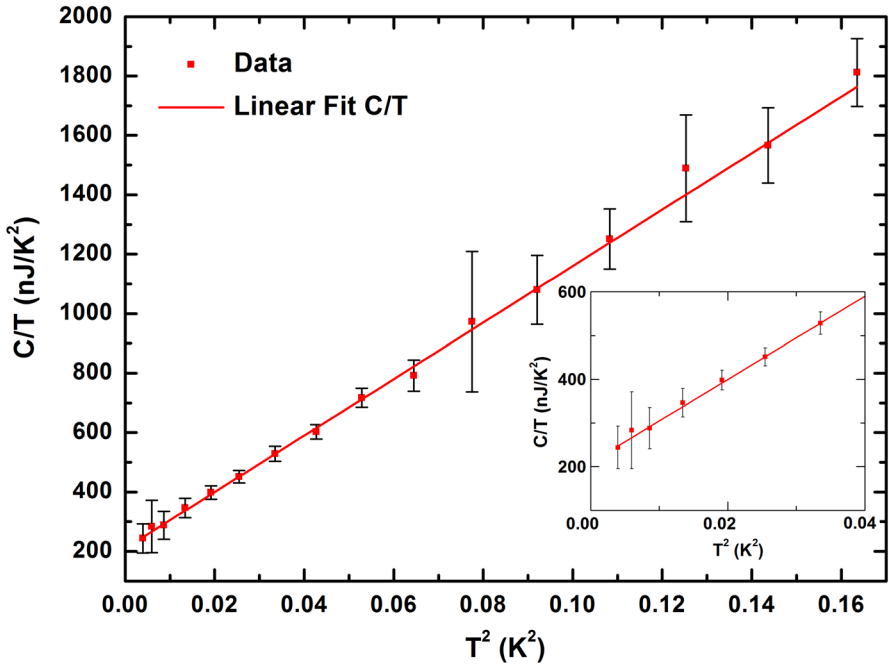


Fig. 4 The measured heat capacity of  $M_1$  together with addenda. The error bars are due to the standard deviation of the measured time constants ( $\tau$ ) for multiple heat pulses at same base temperature. The inset shows the data from 60–225 mK (Color figure online)

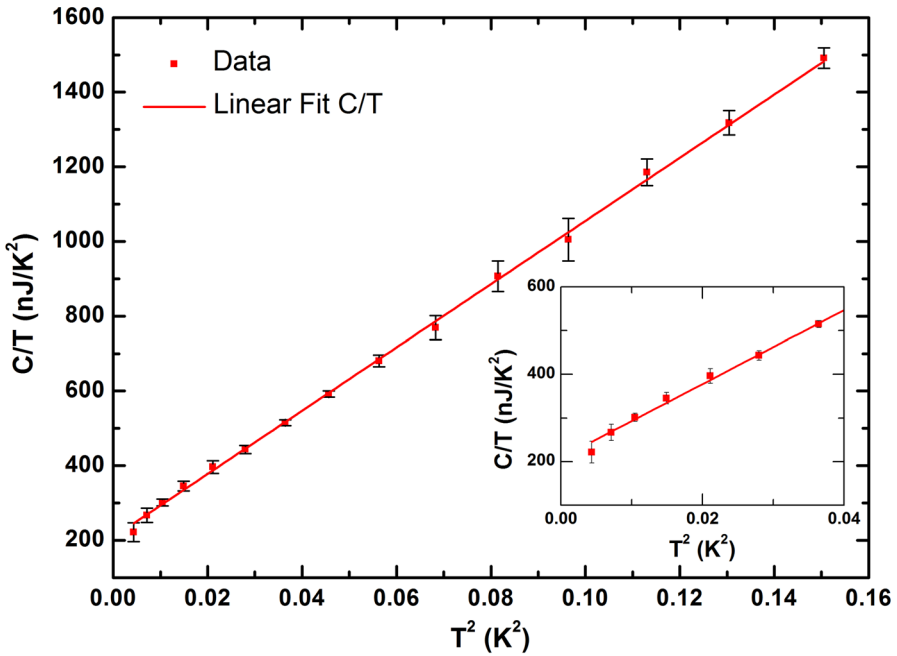


Fig. 5 Same as in Fig. 4 but for  $M_2$  together with addenda (Color figure online)



$$C_{M_2} + C_{addenda} = (209 \pm 3)T + (8464 \pm 69)T^3 \text{ nJ/K} \quad (8)$$

The linear term dominates at low temperature and limits the sensitivity of the setup to measure heat capacity at lower temperatures. The constancy of its coefficient in both Eqs. (7) and (8) indicates that the contribution to the linear term is from the platform and not from the sample. By subtracting (8) from (7) we get

$$C_{M_1-M_2} = (1038 \pm 145)T^3 \text{ nJ/K} \quad (9)$$

When normalized to the mass difference the specific heat of superconducting Tin is obtained as  $(2073 \pm 290)T^3 \text{ nJ/K g}$ , which gives the value of  $\Theta_D$  as  $(199 \pm 9) \text{ K}$ . This is consistent with the reported values on Tin obtained by calorimetric measurements at higher temperatures by O'Neal and Phillips [28] ( $\Theta_D = 198 \text{ K}$ ) and Bryant and Kee-son [29] ( $\Theta_D = 200 \text{ K}$ ). This is also in good agreement with the Debye temperature obtained from measurements of the elastic constants of Tin ( $\Theta_D^e = 201 \text{ K}$ ) [30].

## 5 Conclusions

A calorimeter set up has been devised to measure ultra-small heat capacity of superconductors below 400 mK using Carbon sensors made from commercially available Carbon resistors. The setup is inexpensive and uses off-the-shelf low temperature electronics to measure the heat capacity. Specific heat of Tin has been measured on the setup in the range of 60–400 mK and has been found to be in good agreement with the earlier reported values of Tin which corresponds to a Debye temperature of  $\Theta_D = 200 \text{ K}$ . Measurement below 60 mK were limited due to the thermal decoupling of the sapphire platform from the temperature bath in presence of background heating (vibrational noise) and not due to the the cooling of the mixing chamber of the dilution refrigerator. The absence of anomalous heat capacity in the Tin sample at ultra low temperature along with the result of quasiparticle lifetime saturation by Visser et al. suggests that it should be possible to achieve complete thermalization of energy in a Tin bolometer absorber.

**Acknowledgments** Authors would like to thank Dr. Ashwin Tulapurkar for Platinum thin film deposition on the Sapphire platform. Authors also thank Ms. S. Mishra and Mr. M. S. Pose for assistance during the measurements and Mr. K. V. Divekar for helping with the setup.

## References

1. C. Enss, D. McCammon, *J. Low Temp. Phys.* **151**, 5 (2008)
2. P. Gorla, *J. Phys. Conf. Ser.* **375**, 042013 (2012)
3. C. Arnaboldi et al., *Astropart. Phys.* **20**, 91 (2003)
4. D.S. Akerib et al., *Phys. Rev. D* **72**, 052009 (2005)
5. G. Angloher et al., *Eur. Phys. J. C* **72**, 4 (2012)
6. L. Cardani, *J. Phys. Conf. Ser.* **375**, 042016 (2012)
7. J.W. Beeman et al., *JINST* **8**, P05021 (2013)
8. E. Cosulich et al., *J. Low Temp. Phys.* **93**, 263 (1993)
9. E. Perinati, M. Barbara, A. Collura, S. Serio, E. Silver, *Nucl. Instrum. Methods A* **531**, 459 (2004)

10. S.B. Kaplan et al., Phys. Rev. B **14**, 4854 (1976)
11. P.J. de Visser et al., Phys. Rev. Lett. **106**, 167004 (2011)
12. N.E. Phillips, CRC Critical Rev. Solid State Sci. **2**(4), 467 (1971)
13. M.K. Bacrania et al., IEEE Trans. Appl. Supercond. **56**, 2299 (2009)
14. D.A. Bennett et al., Rev. Sci. Instrum. **83**, 093113 (2012)
15. V. Nanal, International Nuclear Physics Conference: 2013, EPJ Web of Conferences (in press)
16. F. Pobell, *Matter and Methods at Low Temperatures* (Springer, New York, 1996)
17. R. Bachmann et al., Rev. Sci. Instrum. **43**, 205 (1972)
18. G.R. Stewart, Rev. Sci. Instrum. **54**, 1 (1983)
19. M. Brando, Rev. Sci. Instrum. **80**, 095112 (2009)
20. J.P. Shepherd, Rev. Sci. Instrum. **56**, 273 (1985)
21. R.E. Schwall, R.E. Howard, G.R. Stewart, Rev. Sci. Instrum. **46**, 1054 (1975)
22. H. Tsujii, B. Andraka, K.A. Muttalib, Y. Takano, Phys. B **329–333**, 1552 (2003)
23. N. Samkharadze, A. Kumar, G.A. Cs'athy, J. Low Temp. Phys. **160**, 246 (2010)
24. V. Singh, S. Mathimalar, N. Dokania, V. Nanal, R.G. Pillay, S. Ramakrishnan, Pramana J. Phys. **81**, 719 (2013)
25. S. Riegel, G. Weber, J. Phys. E Sci. Instrum. **19**, 790 (1986)
26. P. Esquinazi, R. König, F. Pobell, Z. Phys. Condens. Matter **87**, 305 (1992)
27. J.R. Olson, Cryogenics **33**, 729 (1993)
28. H.R. O'Neal, N.E. Phillips, Phys. Rev. **137**, A748 (1965)
29. C.A. Bryant, P.H. Keesom, Phys. Rev. **123**, 491 (1961)
30. J.A. Rayne, B.S. Chandrasekhar, Phys. Rev. **120**, 1658 (1960)